Free-Tropospheric Static Stability Controls on Tropical Convection in Moist Environments[1]

Scott W. Powell, *Naval Postgraduate School, Monterey, CA*

1. Introduction

Dependence of tropical maritime precipitation on tropospheric humidity is well understood. Many observational[2,3] and modeling[4,5,6,7] studies have indicated that deepening of tropical convection is most sensitive to water vapor in the lower half of the troposphere.

More recent studies have shown sensitivity of modeled rainfall to lower tropospheric temperature[8].

Onset of the MJO over the Indian Ocean may dependent on changes in the free-tropospheric lapse rate that promote vertical growth of cumulonimbi[9,10].

2. Radar Data

Three datasets were collected during DYNAMO in the central Indian Ocean, and one is the NASA KPOL radar at Kwajalein Atoll. S-PolKa and KPOL were/are dual-polarized. The radar data were used to estimate rain rate.

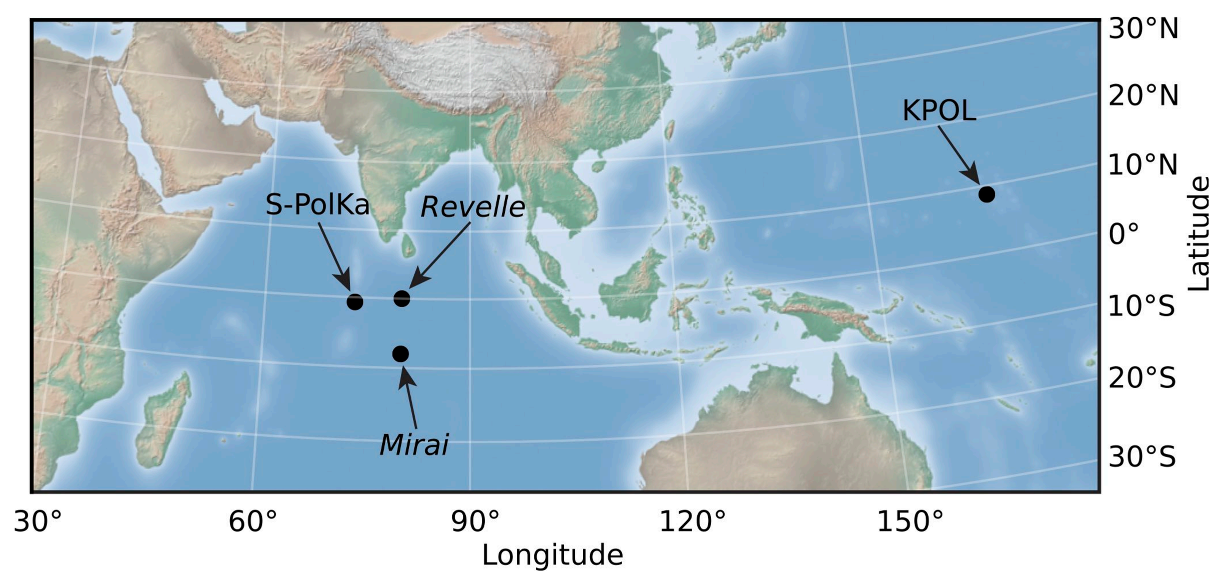

Figure 1: Locations of radars used so far in this study.

Rain-type classification[11] was run on the reflectivity data, and rain rate was computed using dual-pol data if possible[12].

3. Visualizing the Question

Rainfall has been estimated as an exponential function of column-integrated relative humidity (CRH)[13,14], such that

$$CRH = \frac{\int_{P_{sfc}}^{P_{top}} q \, dP}{\int_{P_{sfc}}^{P_{top}} q_{sat}(T) \, dP}$$

CRH is column-integrated specific humidity divided by column-integrated saturation specific humidity.

However, large amount of spread in rainfall exists at high values of CRH (generally ≥ 0.8).

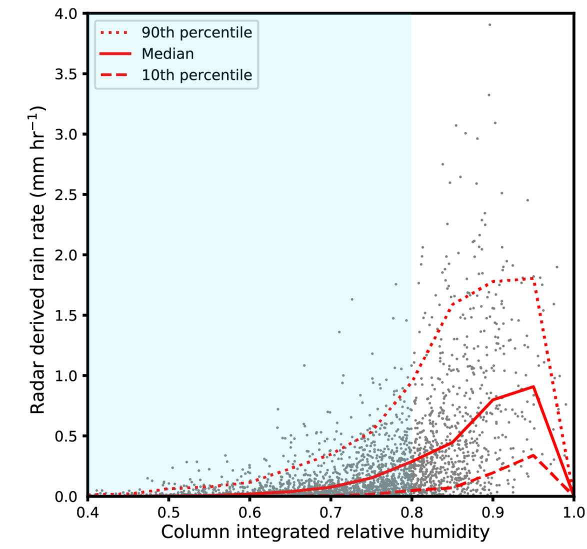

Top, left: CRH vs radar-derived rain rates. The red lines denote the 10th and 90th percentiles of rain rate as a function of CRH.

Bottom, left: Picture taken from R/V Thompson during PISTON on 7 Sept 2018 at 0230 UTC.

Bottom, right: Sounding from 0230 UTC 7 Sept 2018.

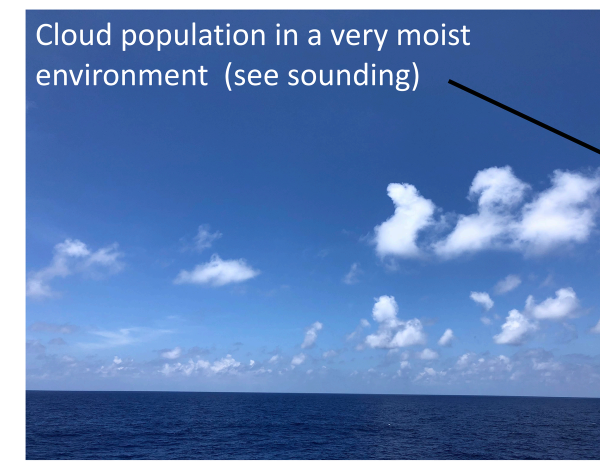

Picture from E. Maloney (Colo. State)

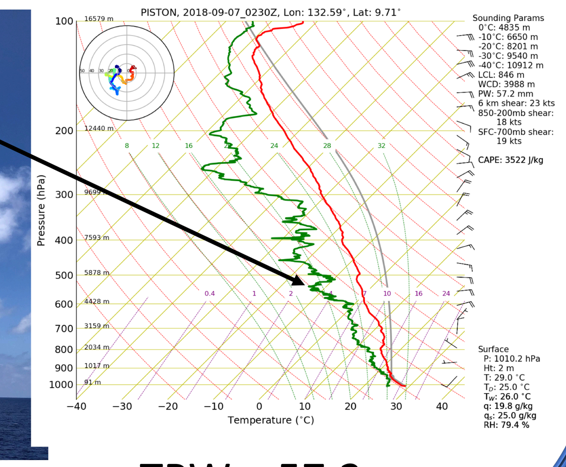

TPW = 57.2 mm

4. Modeling Convection

Ideal simulations using CM1[15]. Horizontal grid spacing of 1 km. Forced based on composite sounding during rainy periods of DYNAMO (red, green below). Lapse rate altered by +/- 3°C/km in 0.5°C/km increments within 100 hPa thick layers from 1000–900 hPa to 200–100 hPa (for 117 model runs).

Domain: 128 km x 128 km, periodic boundary conditions

Full physics, no cumulus parameterization

Right: Mean DYNAMO sounding (red for temperature, green for dew point) during rainy periods (active MJO). Pink represents +/- 1°C/km, and dark green represent corresponding dew point lines with same CRH.

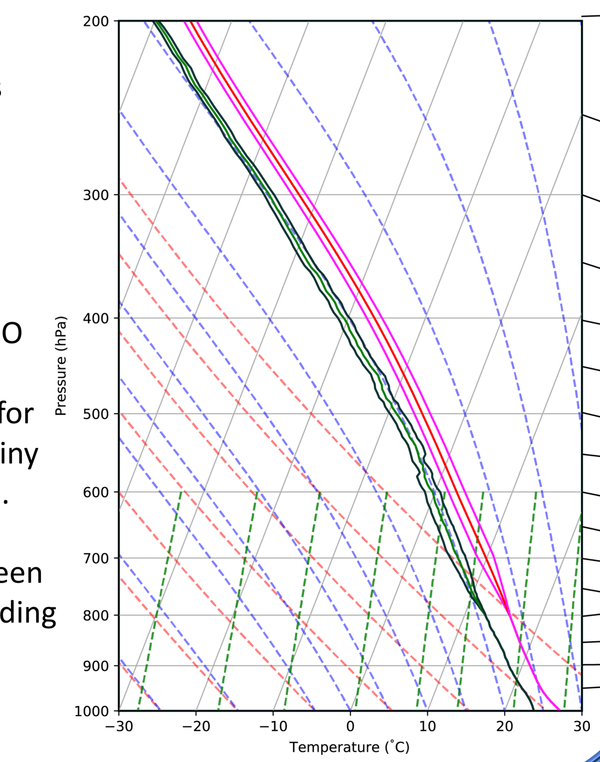

4. Areal Coverage of Precipitation vs. Rain Rate

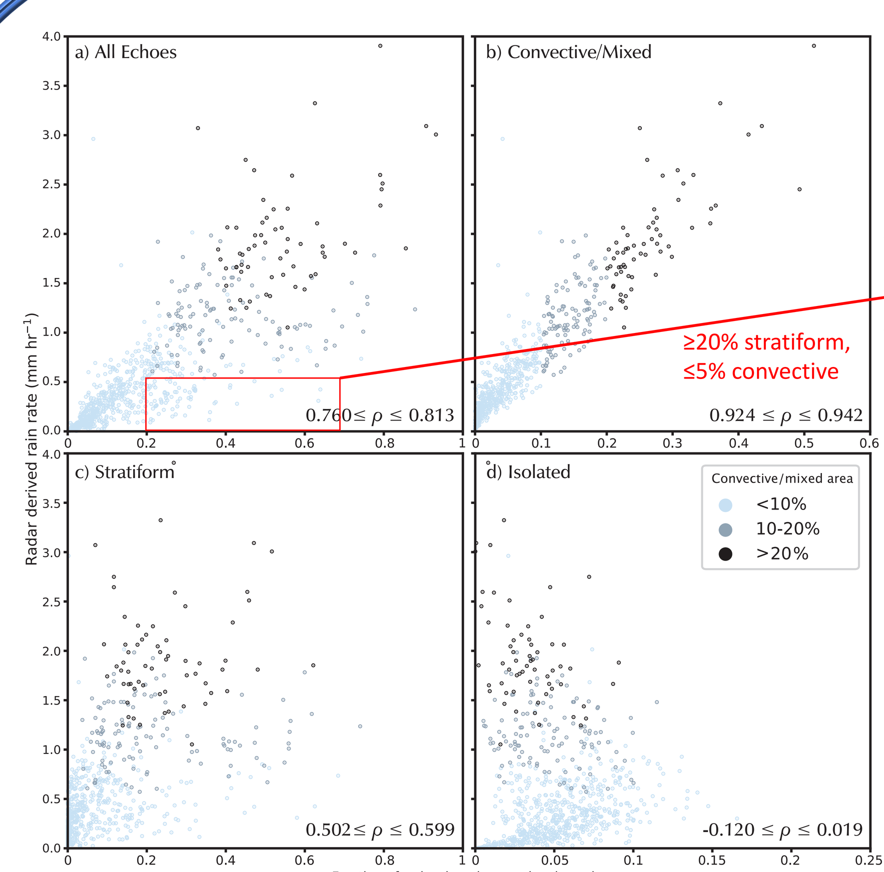

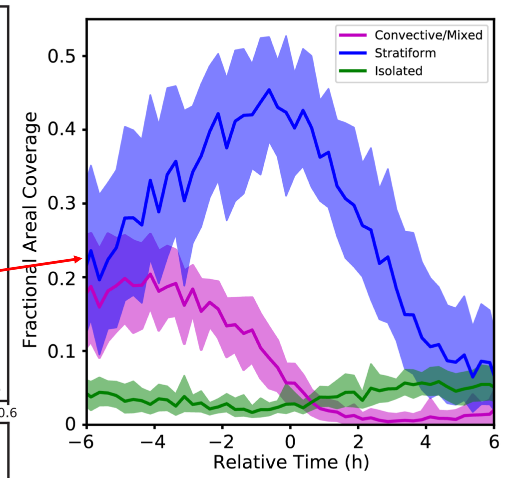

Above: Time series of convective, stratiform, and isolated rainfall relative to the start of a ≥20% stratiform, ≤5% convective period. Low rainfall events occurring during periods of high areal coverage tend to occur when convection decays into stratiform.

Above: Radar-derived mean rain rates as a function of the fraction of the radar domain experiencing precipitation of the type denoted in each panel (reflectivity ≥ 7 dBZ). Darker shades of blue indicate higher area coverages of convective rainfall. The rain rates shown occurred only when CRH exceeded 0.8.

A positive correlation existed between areal coverage of rainfall and domain-mean rain rate. However, even when areal coverage exceeded half the domain (panel a), rain rate ranged from near 0 to near 4 mm hr^{-1}. On the other hand, radar-derived rain rate was strongly correlated with the fraction of the domain experiencing **convective** rainfall.

The part of the convective lifecycle (e.g. early convective or mature stratiform) observed in the radar domain is one factor in the spread of rain rates at high CRH. If echo covers half the domain, but all of the echo is stratiform, then radar-domain mean rain rate will be small. However, sometimes total areal coverage is near 0. What causes little to no echo to occur when CRH is high?

5. Environmental Characteristics

Rawinsonde data were co-located with each of the radar datasets. I used these data to compute kinematic and thermodynamic properties of the troposphere. Rawinsonde data was matched with radar data collected within 1.5 hours of launch.

Left: Mean sounding profiles during upper quartile of echo areal coverage minus mean profiles during the lower quartile. The colored lines denote results from different sites, and the black line is the composite. Shading represents the 95% confidence interval.

Below, right: 900–700 hPa lapse rain vs radar-derived rain rate, color coded by the quartile of convective rainfall. Only a small correlation exists.

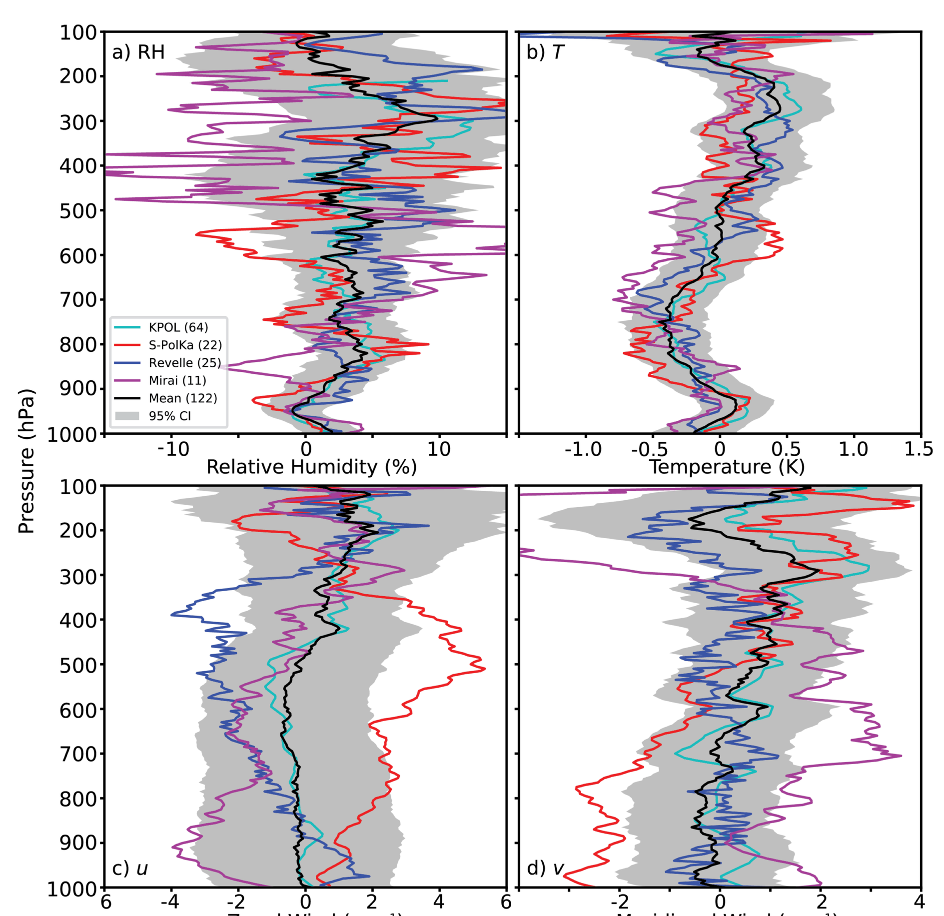

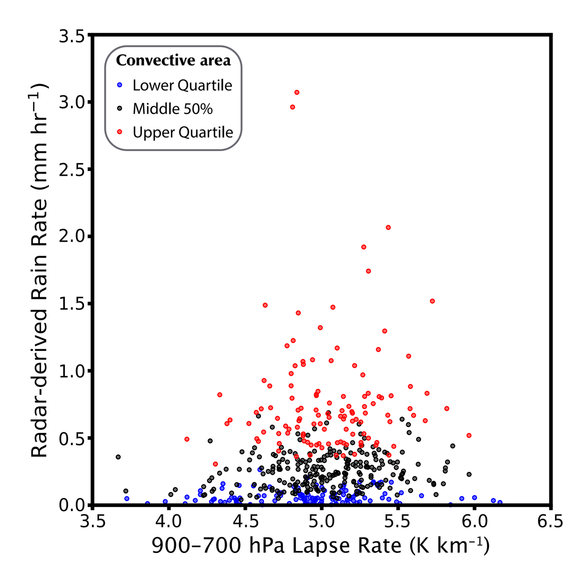

Bottom: Table derived from ERA-I reanalysis of SST and SST gradient at the radar site during times when echo areal coverages were less than (greater than) low and high quartiles.

	SST (low) (K)	SST (high)	ΔSST (low) (K km^{-1})	ΔSST (high)
S-PolKa	[302.03,302.08]	[302.04,302.10]	[7.96,8.54]e-4	[7.67,8.44]e-4
Mirai	[302.10,302.26]	[302.13,302.27]	[1.72,1.93]e-3	[1.75,1.94]e-3
Revelle	[301.95,302.00]	[301.96,301.99]	[4.85,5.95]e-4	[5.09,6.35]e-4
KPOL	[302.01,302.08]	[302.03,302.11]	[1.70,1.85]e-3	[1.69,1.85]e-3

6. Modeling Results

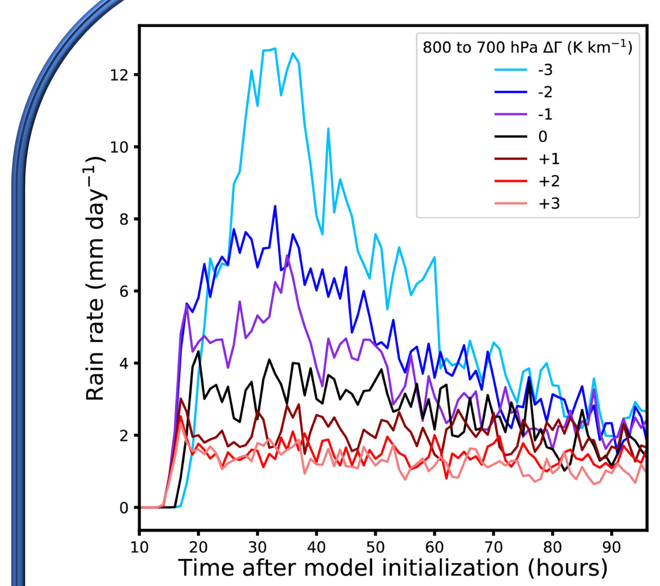

Above: Domain-mean rain rate as function of time in CM1 simulations for soundings with lapse rate changed between 800 and 700 hPa.

All simulations approach a similar equilibrium by 24 hours after initialization. Simulations with largest destabilization in forcing experience largest rain rate about 8 hours after initialization.

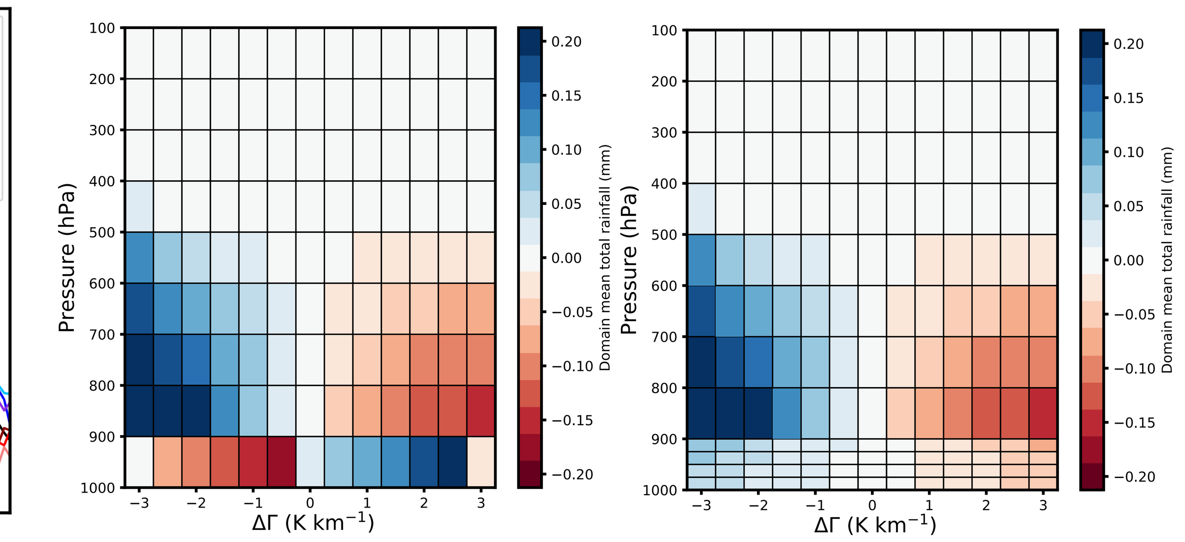

Domain-averaged 24-hour rainfall totals for sounding with lapse rate varied by the amount shown on the abscissa in the pressure layer shown on the ordinate. Right: Same as left, but with 25-hPa deep layers below 900 hPa.

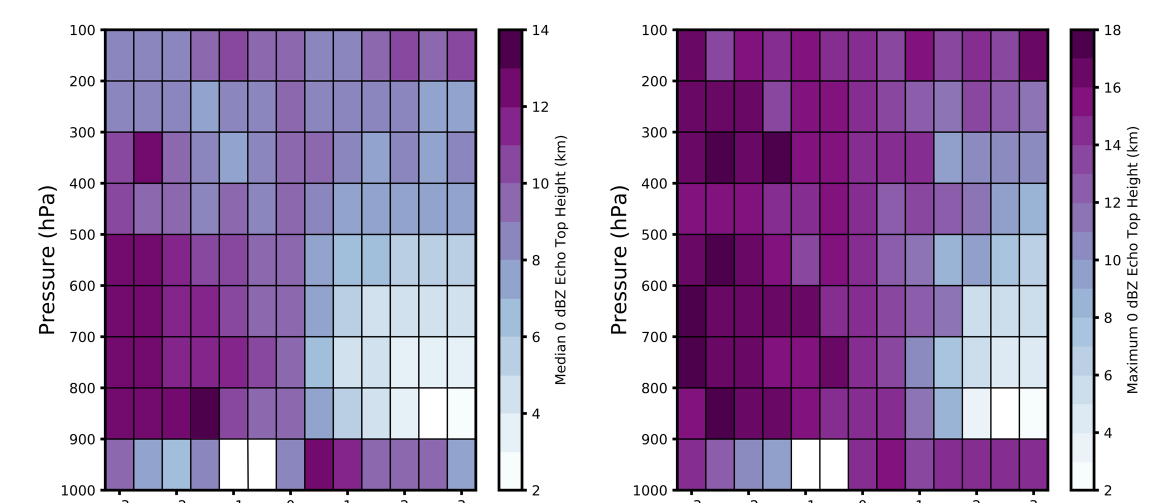

These figures are read the same way as the red and blue ones above. Left: Median 0 dBZ "echo" top height. Right: Maximum 0 dBZ "echo" top height.

Changing the lapse rate at all levels below 500 hPa impacts rain rate and depth of modeled convection.

The depth of the layers altered in the sounding used for forcing is important too. Notice the different results in the boundary layer when changing the lapse rate within 100 hPa vs. 25 hPa deep layers.

[1] Powell (2019), *JAS*, **76**, 3737–3751, doi:10.1175/2019-JAS-D-0144.1
[2] Brown and Zhang (1997), *JAS*, **54**, 2760–2774
[3] Powell and Houze (2013), *JGR-Atmos.*, **118**, 11979–11995, doi:10.1002/2013JD020421
[4] Derbyshire et al. (2004), *QJRMS*, **130**, 3055–3079, doi:10.1256/qj.03.130
[5] Muller et al. (2009), *JGR-Atmos.*, **36**, L16804, doi:10.1029/2009GL039667
[6] Kuang (2010), *JAS*, **67**, 941–962, doi:10.1175/2009JAS3260.1
[7] Wang and Sobel (2012), *JGR-Atmos.*, **117**, doi:10.1029/2011JD016847
[8] Tian and Kuang (2019), *JAS*, **76**, 27–41, doi:10.1175/JAS-D-18-0023-1
[9] Powell and Houze (2015), *JGR-Atmos.*, **120**, doi:10.1002/2014JD022961
[10] Powell (2016), *JAS*, **73**, 2913–2934, doi:10.1175/JAS-D-15-0326-1
[11] Powell et al. (2016), *J Tech.*, **33**, 523–538, doi:10.1175/JTECH-D-15-0135.1
[12] Thompson et al. (2018), *JAMC*, **57**, 755–775, doi: 10.1175/JAMC-D-0160.1
[13] Bretherton et al. (2004), *J. Climate*, **17**, 1517–1528
[14] Rushley et al. (2018), *GRL*, **45**, 1133–1140, doi:10.1002/2017GL076296
[15] Bryan and Fritsch (2002), *MWR*, **130**, 2917–2928

This poster was supported by Research Initiation Program funding from the Naval Postgraduate School.